ACS OMEGA

Open Access

http://pubs.acs.org/journal/acsodf

Article

Waste Algal Biomass as a Binder for Shaping Technical Adsorbents

Eduardo Perez-Botella, Yesid S. Murillo-Acevedo, Bárbara Bastos de Freitas, Kyle J. Lauersen, and Carlos A. Grande*

Cite This: *ACS Omega* 2025, 10, 17735−17743

Read Online

ACCESS | Metrics & More | Article Recommendations | Supporting Information

ABSTRACT: Spray-dried biomass from genetically engineered *Chlamydomonas reinhardtii* can be used as a binder to extrude alumina adsorbents. The proposed process involves heating at a moderate temperature (180 °C), replacing inorganic binders that require high sintering temperatures. The transformed genes present in the algal biomass were no longer detectable after the thermal treatment. Binder contents above 15% led to successful extrusion. Extrudability was found to correlate with the viscoelasticity coefficient, tan(δ), obtained from independent rheometric measurements. The extrudates have crush strengths of >27 N, complying with industrial requirements. The water vapor adsorption capacity in shaped alumina adsorbents was 7.5 mol/kg, indicating a 30% reduction compared with alumina powder. The mechanical and adsorption properties of the formed adsorbents remain unaltered after a 1 week immersion in water, ethanol, or *n*-heptane and after 10 gas-phase adsorption/desorption cycles. The results demonstrate that waste biomass from algal processes can be effectively used to produce functional industrial adsorbents.

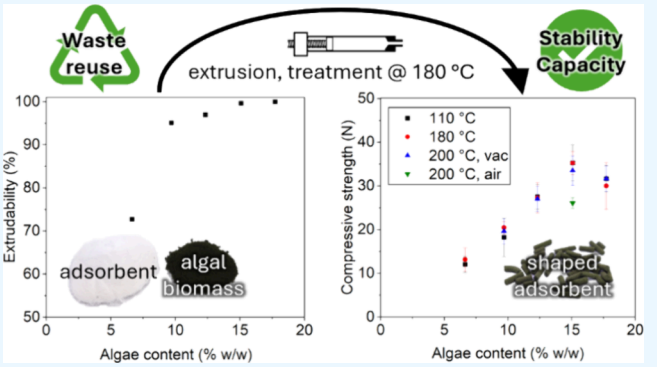

INTRODUCTION

Adsorbents are porous materials with a high surface area that develop specific interactions with one species from a mixture. Adsorbents are used in numerous important separation and purification processes, such as water purification or drying of gas and liquid streams.[1] Adsorbents are frequently produced as powders (μm scale). To avoid excessive pressure drop when used in industrial large-scale applications, they need to be agglomerated into larger particles (mm scale).[2]

There are different technologies for shaping adsorbents and catalysts, such as pelletization, granulation, coating, casting, foaming, spinning, 3D-printing,[3,4] and extrusion.[5,6] Extrusion is one of the leading shaping technologies,[2] as production is fast and different shapes can be achieved with the same infrastructure.

Different types of extruding systems are shown in Figure 1A. The adsorbent needs to be mixed to form a paste that possesses certain rheological properties (Figure 1B). This paste normally contains the adsorbent, binders, and plasticizers.[7,8] The binder provides cohesion and mechanical stability to the final adsorbent bodies. Binders can be organic or inorganic and temporary or permanent, depending on whether they are removed at some stage of production. Plasticizers make the paste malleable and ultimately extrudable. Water is the most common plasticizer, but additives like cellulose derivatives can be added to improve cohesion and to avoid phase separation.[9] Some materials can act as both a binder and a plasticizer. After being mixed and kneaded, the paste is extruded, producing an elongated "wet" body. The paste fed to an extruder typically contains 20−60% adsorbent, 2−30% binders, and 20−50% water. The extruded body is then cut to the desired length and dried, resulting in the "green" adsorbent body. Finally, it is subjected to a thermal treatment that removes water and eventually improves the mechanical properties. The heating can also be termed "firing".[2] Organic additives leave pores in the final material after firing, thus acting as pore-forming

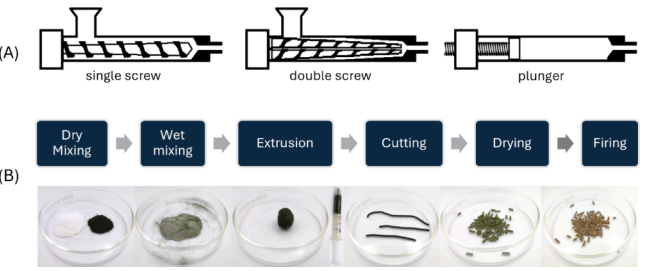

Figure 1. Different extruder types (A) and steps required for shaping through extrusion (B).

Received: January 7, 2025
Revised: February 16, 2025
Accepted: April 14, 2025
Published: April 23, 2025

agents. The final material contains 30−95% of the adsorbent, the rest being binders. The final thermal treatment must be adapted for adsorbents with low thermal stability, such as silica gel and metal−organic frameworks (MOFs),[10] covalent organic frameworks (COFs),[11] or where the permanent binder is organic.

With the final aim of enhancing the sustainability of chemical processes, all steps of manufacturing should be optimized, including adsorbent shaping. There are several strategies to reduce the environmental impact of the shaping process:

- decreasing the energy required for thermal treatment,
- reducing the amount of (pre)processing steps to the minimum, and
- replacing one or more starting materials by waste products from another process.

Any modified shaping process should produce an adsorbent with the same or similar properties as that prepared with existing technology. Moreover, the reusability of the shaped adsorbent is also important, and any improvement in points i−iii should not come at the expense of a loss in the final material's lifespan.

Waste or secondary products from other processes have been tested as replacements for pore-forming agents or raw materials in ceramics[12] or as feedstock for adsorbent synthesis.[13] Pretreatment of these wastes using resource- or energy-intensive processes decreases the overall sustainability of adsorbent manufacturing. Materials produced in processes complying with points i−iii are more interesting for future implementation; however, the published literature is currently scarce. Hamd et al. produced a seaweed-zeolite nanocomposite by impregnation, which exhibited enhanced dye removal performance as compared to the bare zeolite.[14] Yang et al. used crude algal biomass from the green alga *Chlamydomonas reinhardtii* to produce thin-film composite membranes on cellulose supports.[15] Nakanishi et al. have used the same algal biomass as a raw material in bioplastic production.[16] Developing new solutions in this area could lead to discoveries in the manufacturing of shaped adsorbents, catalysts, and other shaped bodies used in chemical industries.

The microalga *C. reinhardtii* has been investigated for its prospects in the sustainable production of hydrogen and other chemicals mediated through emerging genetic engineering strategies.[17] The alga can be used to produce tailored chemicals while conducting wastewater treatment, making it an attractive waste-reuse vehicle.[18] Global regulations vary on the use of engineered whole cell biomass as a food additive, while purified isolated chemicals from engineered organisms are accepted as produced.[19] Processes using engineered algae to generate tailored products may lead to the production of algal biomass separate from the target chemical or cleaned water.[18,20] The biomass is composed of protein, carbohydrates, lipids, and pigments and can also be further valorized through several approaches. Separating individual chemical components from the biomass requires dedicated downstream processes that are generally not economically viable. Uses of waste algal biomasses that involve applications of the whole cell material are more economically attractive.[15,16] Another approach involves the production of algal biochar through pyrolysis.[21]

Algae are diverse, and their biochemistries are varied. However, the mechanical properties displayed by bioplastics derived from *C. reinhardtii* are comparable to those of polymers like polybutylene succinate and low-density polyethylene,[16] which can be used as binders in adsorbent formulations.[22] Additionally, the hydrophilicity shown by algal biomass[16] indicates it might be used as a binder or a plasticizer similar to hydrophilic polymers, such as cellulose[22] or methylcellulose.[8]

In this work, genetically engineered *C. reinhardtii* biomass waste was used as a binder in the formulation of extruded alumina adsorbents for the first time. This opens a new path for the valorization of this type of waste with a reduced number of intermediate steps. The extrudability and rheological properties of different algae-alumina pastes are studied as a function of the algal biomass content, and confirmation of genetic material destruction is shown. The influence of the paste composition and the thermal treatment conditions on the mechanical and adsorption properties of the extrudates is rationalized. Shaping using algal biomass waste is presented as a novel, low-energy, and environmentally friendly process for the manufacture of technical adsorbents for low-temperature applications in gas and liquid phases.

MATERIALS AND METHODS

Algae Biomass. *Chlamydomonas reinhardtii* strain UPN22[23] transformed with the pOpt3_mVenus_Paro plasmid[24] was cultivated by Algae 4 Future (A4F, Portugal) throughout 2023. Multiple cultivation rounds were conducted throughout the year in 1000 L tubular photobioreactors in the A4F greenhouse, and the resulting biomass was spray-dried to generate a powder. *C. reinhardtii* residues were delivered to KAUST in room-temperature vacuum-sealed bags. The extrusion was done using a batch of algae waste referred to as batch 1 in the Supporting Information (SI). Samples were stored in air at 60% relative humidity (RH) and 21 °C for 5 months after unsealing. The algal biomass was crushed in a mortar and pestle for 2 min prior to its use, except if indicated otherwise.

Adsorbent Formulation Extrusion. Dry mixing of powder activated alumina (neutral, Brockmann I, Sigma-Aldrich) and algal biomass was performed in a mortar for 1 min. Deionized water (Milli-Q) was added, and the mixture was kneaded, ensuring a homogeneous paste. At this stage, the extrudability of the paste was studied (see below), and part of the paste was reserved for rheometric measurements.

The extrusion of the paste was performed using plunger extruders. Two different chamber sizes were employed: (1) a small chamber with 8.6 mm internal diameter and 3 mL nominal volume and a cylindrical dye with 1.80 mm diameter and (2) a larger chamber with 26.6 mm internal diameter and 60 mL nominal volume and a cylindrical dye with 2.08 mm diameter. The plungers produced an elongated wet cylindrical extrudate at speeds of 0.5−5 cm/s. The extrudates were left to dry for 16 h at 60% RH and 21 °C until they were broken into smaller (≈0.5 cm) pieces. Thereafter, the shaped extrudates were dried at 110 °C for 12 h. Additional thermal treatments at higher temperatures were also performed as indicated in the forthcoming sections. Modifications to this reference procedure were tested to study the robustness of the production method (SI, section 2.9). The extrudates are named as "Al_2O_3−Alg#", where "#" is the mass percentage of the binder in the dry material, and a suffix "_nc" is added to samples prepared with noncrushed algae.

https://doi.org/10.1021/acsomega.5c00173
ACS Omega 2025, 10, 17735−17743

Weathering of Extrudates. Given that alumina is used in liquid- and gas-phase adsorption processes,[1] the extrudates were subjected to weathering experiments emulating possible usage conditions. The objective, particularly for the liquid systems, is to see whether there is severe physical deterioration of the samples after being in contact with certain chemicals. For the gas-phase weathering, refer to the section on adsorption methods below. For the liquid-phase weathering, the formulated extrudates were submerged for 1 week in independent sealed containers containing different chemicals: (1) water, (2) ethanol/water 96:4 w/w, (3) heptane, and (4) paraffin oil. After the immersion period, all of the extrudates were dried at 110 °C for 12 h. The extrudates soaked in paraffin oil underwent a prior wash with acetone before the drying step to remove the oil. The sample was additionally treated in air at 200 °C for 8 h to remove as much oil as possible.

Physicochemical Characterization of Raw Materials. Thermogravimetric analysis (TGA) was conducted on a TGA 5500 instrument (TA Instruments) under a nitrogen flow of 150 mL/min. The sample was heated to 3 °C/min. Elemental analysis was carried out in a Thermo Flash 2000 instrument (Thermo Fisher Scientific). In CHNS determination, the combustion took place in an oxygen atmosphere at 950 °C. The oxygen (O) determination was carried out under a He atmosphere at 1060 °C. Quantitative analysis of other elements was done by X-ray fluorescence (XRF) in a Bruker S8-Tiger Wavelength Dispersive XRF spectrometer. A sample holder lined with a polymer film (prolene 4 μm thin film) was used, and each sample was analyzed in duplicate. The materials' particle size and morphology were studied by scanning electron microscopy using an FEI TENEO microscope (Thermofisher). The structural characterization of alumina was done by X-ray diffraction (XRD) using a Bruker D2 Phaser diffractometer with Cu−Kα radiation (λ_1 = 1.5405 Å).

Biochemical Characterization of Algal Biomass. The total carbohydrate and protein contents were determined from an algal extract prepared in Milli-Q water, while the total lipid content was measured using an algal extract prepared in chloroform−ethanol (1:2, v/v). Pigment composition was analyzed from algal extracts prepared in 80% acetone. For all *C. reinhardtii* strain UPN22 extracts, the intracellular material was released using a bead beating at high speed for three 60 s intervals (FastPrep-24 5G, MP Biomedicals), using tubes with Lysing Matrix D (MP Biomedicals). Carbohydrate content was quantified using the phenol-sulfuric acid method with a standard glucose curve.[25] Protein content was determined using a colorimetric method followed by thermal and alkaline pretreatment. Total lipids,[26] chlorophyll a and b,[27] and total carotenoid[28] contents were determined. Absorbance readings for pigment analysis were taken from the acetone extracts at 470, 645, and 663 nm.

Genomic DNA was extracted from the spray-dried *C. reinhardtii* strain UPN22 using the Zymo Quick-DNA fungal/bacterial extraction kit (Zymo Research Group, USA). DNA extracts were then quantified using a NanoDrop One spectrophotometer (Thermo Fisher Scientific, USA). To assess whether the DNA remained intact after the thermal treatments were applied, we amplified the genes with the primers listed in Table S1. Polymerase chain reactions (PCRs) were carried out in a volume of 25 μL using Phusion Green Hot Start II High-Fidelity PCR Master Mix (Thermo Scientific).

Extrudability. Some pastes undergo phase separation when force is applied on them.[9] This leads to a more fluid phase being extruded and a more solid phase remaining stuck inside the extruder. The extrudability (η_{ext}) of the different pastes is defined as

$$\eta_{ext} = \frac{m_{ext}}{m_t - \rho_p V_d} \quad (1)$$

where m_{ext} is the mass of the extruded fraction, m_t is the total amount of paste introduced in the plunger, and $\rho_p V_d$ is a correction to account for the material fraction with density ρ_p remaining inside the system's dead volume (V_d). This equation is valid only if the total volume of the paste is larger than the dead volume. In the case where there is physical separation into two phases, it is assumed that only the water content changes, but the alumina/binder ratio remains constant (Table S5). The masses of the total and extruded fractions were determined by weighing. The paste density and the dead volume were determined as described in the SI, section 2.6.

Rheological Properties. The rheology of the extrusion pastes was studied by using an AR-G2 rheometer (TA Instruments). The rheological characterization of extrusion pastes gives information on the viscoelasticity and flow properties that define the behavior during extrusion. Oscillatory experiments were done to determine the viscoelasticity coefficient tan $\delta = G''/G'$ and the yield stress σ_y. The primary parameters are the storage or elastic modulus G' (a measure of the energy stored upon deformation) and the loss or viscous modulus G'' (a measure of the energy transformed to achieve deformation). The yield stress gives the minimum stress at which the material starts deforming. Rotational or flow experiments were used to determine the shear stress, the shear rate, and the dynamic viscosity. The dynamic viscosity gives information on how the material resists deformation. More information can be found in the SI, section 1.2.

Mechanical Stability of the Extrudates. The mechanical strengths of the extrudates dried at 110 °C, the ones treated at 180−200 °C, the ones subjected to multiple gas-phase adsorption cycles, and the ones weathered in different solvents were characterized. A Zwick-Roell TeachXPert universal tester was used to measure the crush strength. International standard ISO-604-1993 was used as a guideline.[29] For each material, six independent analyses were performed, and the average was reported. The material was placed with its longest dimension on the testing surface.

The crush strength is defined as the maximum force measured (F) before a substantial decrease (>30% of the maximum) is recorded. The compressive stress at break (σ_b) is calculated as the quotient between the crush strength and the maximum cross-sectional area (A):

$$\sigma_b = \frac{F}{A} = \frac{F}{d \cdot l} \quad (2)$$

where d and l are the specimen diameter and length, respectively. The average stress at break was used to calculate the hypothetical crush strength of a cylinder with dimensions of l = 5 mm and d = 2 mm.

Adsorption. The materials were studied through N_2 adsorption at −196 °C using an ASAP 2420 (Micromeritics) to determine the Brunauer−Emmett−Teller (BET) surface area[30,31] and to determine their pore size distribution

https://doi.org/10.1021/acsomega.5c00173
ACS Omega 2025, 10, 17735−17743

Table 1. Sample Formulated and Dry Compositions, Extrudability in a Large Plunger (LP) and a Small Plunger (SP), and Dry Material Yield

sample	water in paste (%)	alumina, dry basis (%)	algae, dry basis (%)	extrudability LP (%)	extrudability SP (%)	yield (%)
Al_2O_3–Alg7	34	93	7	72	73	58
Al_2O_3–Alg10	33	90	10	94	95	83
Al_2O_3–Alg12	32	88	12	93	97	85
Al_2O_3–Alg12_nc	31	88	12	74	84	61
Al_2O_3–Alg15	32	85	15	93	100	87
Al_2O_3–Alg18	31	82	18	100	100	91

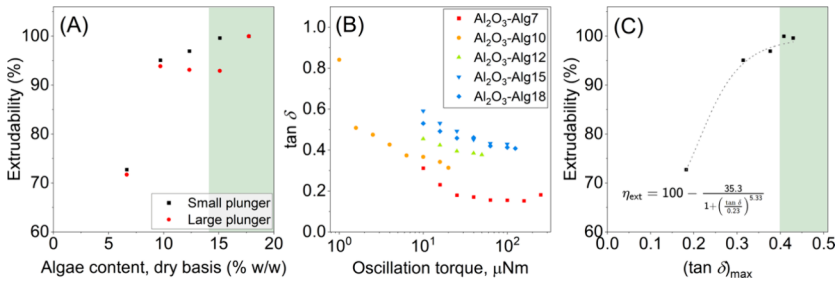

Figure 2. Extrudability as a function of algal biomass content in the dry solid (A), viscoelasticity coefficient tan δ of the different pastes as a function of oscillation torque (B), and extrudability plotted against the viscoelasticity coefficient tan δ measured at the highest torque within the linear viscoelastic region (C).

according to the Barrett–Joyner–Halenda method.[32] The samples were activated at 200 °C under vacuum for 8 h. An activation temperature of 200 °C held for 40 min is sufficient for both the powder alumina and the extrudates. Higher temperatures are not required for the regeneration of the alumina (see section 2.5 in the SI) and can be detrimental to the integrity of the extrudates, as will be seen below.

Water vapor adsorption using a Hiden IGA Moisture Sorption gravimetric device was used as the method for determining adsorption capacity and kinetics. The adsorption properties of the extrudates produced in different conditions were investigated by comparing single point measurements of adsorption of water vapor at 25 °C and 90% RH using nitrogen as the carrier gas. Activation was performed at 200 °C in a N_2 flow for 40 min. To test the extrudates, 11 cycles of adsorption–desorption of water vapor at 25 °C were performed. Adsorption was performed with a stream containing 90% water vapor at 25 °C. Two types of desorption strategies were tested: (1) heating to 120 °C for 60 min and (2) heating to 200 °C for 40 min. An estimation of the diffusional time constant using the linear driving force (LDF) approach was performed (SI, section 1.3).

RESULTS AND DISCUSSION

Characterization of Algal Biomass and DNA Content Analysis. The composition of the spray-dried biomass from the *C. reinhardtii* strain UPN22 is shown in Figure S1. As this is a genetically modified strain of algae, it was important to determine if DNA survived the extrudate production procedure, posing a risk of genetic escape. The DNA content was reduced by 85.9 and 99.3% upon treatment at 110 and 180 °C, respectively, compared to packaged biomass, indicating destruction of DNA by this treatment (Table S3). The inactive nature of the remaining DNA was confirmed by the absence of signals in PCR for either antibiotic resistance or mVenus reporter genes that had previously been transformed into this strain (Figure S2). The results indicate that the thermal treatments performed on the algal residues are enough for safe utilization as a binder for the extrusion of adsorbents.

The thermal behavior of *C. reinhardtii* biomass (Figure S3) showed several decomposition stages, which are discussed in detail in the SI, section 2.2.2. *C. reinhardtii* biomass treated at 180 °C presents only a loss of moisture below 120 °C and no significant loss up to 200 °C, which means that the treatment stabilized the biomass significantly. Small differences were observed between different algal biomass batches (Figure S3A). Samples analyzed in air or nitrogen (combustion vs pyrolysis) show no differences under 280 °C (Figure S4B).

Crushing reduced the average particle size of algal biomass from (64 ± 51) to (19 ± 18) μm (Figures S5A,B and S6A). The particle size and shape achieved by crushing were reproducible between biomass batches and were maintained after treatment at 180 °C (Figure S7).

Characterization of Alumina. The particle size of alumina was found to be (89 ± 36) μm (Figures S5C,D and S6B). The particles are shaped like compact irregular polyhedra. The XRD pattern measured for the alumina corresponds to γ-Al_2O_3[33] (Figure S8), but with an additional low-intensity peak at 43°, revealing a very small amount of α-Al_2O_3. Alumina shows an S-shaped, Type IV(a) nitrogen adsorption isotherm (Figure S9), and a BET surface area of 163 m^2/g, which is within the supplier's specification (150 ± 15) m^2/g. The BET surface area of commercial alumina can vary from 100 to 400 m^2/g.[34−36]

Extrudability and Rheological Properties. Sample compositions, extrudabilities (eq 1), and yields, defined as the dry extrudate mass divided by the total dry solid mass used in the formulation, are listed in Table 1. The dry materials contained 82–93% alumina and 18–6.6% algal biomass. In our case, the density of the paste was (1.69 ± 0.04) g/cm^3 and the dead volumes were (0.045 ± 0.003) and (0.27 ± 0.03) mL for the small and large plungers, respectively (SI, section 2.6).

The extrudability increases with the algae content (Figure 2A). A steep increase in extrudability was observed when the binder content increased from 7 to 10%. Adequate grinding of

https://doi.org/10.1021/acsomega.5c00173
ACS Omega 2025, 10, 17735−17743

the algal biomass and immediate extrusion after paste preparation (SI, section 2.9) were essential to guarantee extrudability. The paste Al_2O_3−Alg12_nc, prepared with the noncrushed algal biomass, presented a much lower extrudability than Al_2O_3−Alg12. Algae contents >15% produced fully extrudable pastes, where the "non-extrudable" fraction from the large plunger could be completely extruded in the small plunger. The dry material yield follows a trend similar to that of the extrudability (see Table 1).

The rheological properties of pastes containing different amounts of algal biomass have a direct effect on the extrudability of the paste (Figure 2B). A torque sweep in the linear viscoelastic region was used to determine the viscoelasticity coefficient tan δ of each paste. All samples presented tan δ values between 0.1 and 1, which indicates that all samples were more elastic than viscous. The viscoelasticity coefficient showed a decrease as the torque increased, and pastes with higher extrudability showed overall higher values of tan δ. The complete set of rheological results can be found in the SI, section 2.7.

By plotting the extrudability in the small plunger against the viscoelasticity coefficient obtained at the highest torque assessed for each paste, we find that the correlation between these two magnitudes becomes evident (Figure 2C). Assuming a logistic relationship in the studied region, the fit gives an R^2 of 0.992. Herewith, we demonstrate that a very simple and fast experiment (torque sweep in the linear viscoelastic region) can be used to determine whether a mixture can be extruded or not. In the case of algae−alumina−water mixtures, full extrudability is achieved with pastes with a $(\tan \delta)_{max} \gtrsim 0.4$. For this system, full extrudability is achieved when the algal biomass content is higher than 15%.

Mechanical Properties of the Extrudates. The mechanical strength of the extrudates was studied after treatment at 110−200 °C in air or at 200 °C in vacuum (Figure 3). The compressive strength increases with the algae

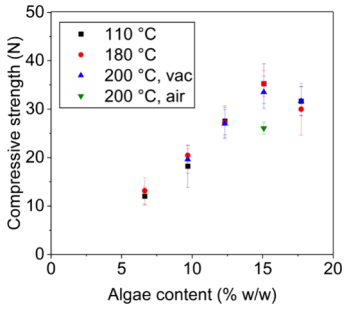

Figure 3. Compressive strength vs algae content after different thermal treatment conditions.

content until it reaches a plateau at 15% w/w. These values correspond to compression stresses of 3−3.5 MPa, close to those of commercial adsorbents (Table S2). The difference in mechanical strength between particles treated at 110 and 180 °C in air or 200 °C under vacuum was only minor in every case, whereas higher temperatures in air caused a very substantial decrease in mechanical stability accompanied by a change in color from olive to brown. Additionally, a variability of 5−10 N can be expected if different batches of algal biomass are used (SI, section 2.9).

Adsorption and Textural Properties. The samples displaying compressive strength >18 N and high extrudability were further characterized by water vapor sorption at 25 °C and N_2 adsorption at −196 °C. By measuring a 1-point water vapor sorption isotherm at 90% RH and fitting the uptake curve to the LDF model (Figure S15), we can compare the adsorption capacities and diffusional time constants (Figure 4

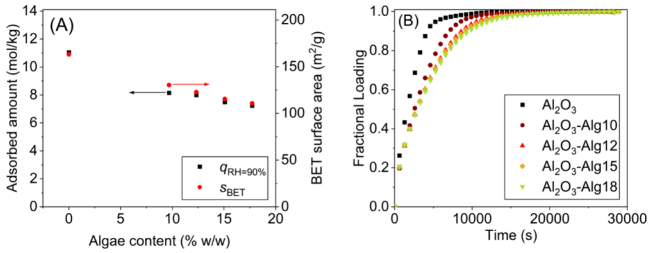

Figure 4. Experimental adsorption capacities at 90% RH and BET surface areas as a function of the algal biomass content in the extrudates (A) and uptake curves of the different materials compared to those of the parent alumina (B).

Table 2. Evolution of the BET Surface Area, Adsorbed Amounts of Water at 90% RH and 25 °C, and Diffusional Time Constants with the Amount of Binder

			RH = 90%, 25 °C		
sample	algal biomass content, dry basis (%, w/w)	BET surface area (m^2/g)	q_∞ (mol/kg)	$t_{0.95}$ (h)	D/r^2 (10^{-5} s^{-1})
Al_2O_3	0	163	11.04	1.48	3.66
Al_2O_3−Alg10	10	130	8.16	2.38	2.30
Al_2O_3−Alg12	12	123	8.00	2.96	1.87
Al_2O_3−Alg15	15	115	7.49	3.10	1.79
Al_2O_3−Alg18	18	111	7.24	3.38	1.63

and Table 2) of the different samples as a function of algal biomass content. The adsorption capacity showed a decrease as the algal biomass content increased (Figure 4A). The adsorption capacity of the adsorbent was expected to decrease based on the alumina content (Figure S13), but an additional 18% drop in adsorption capacity was observed. That difference indicates that the presence of the algae alters the adsorption properties of the alumina, probably by partially obstructing the pores. The time to reach 95% of the equilibrium sorption capacity increased from 1.5 to 3.4 h when comparing powder alumina and extrudates. The estimated LDF model diffusional time constant decreased by a factor of 2 when the algae content was 15% w/w compared to the bare alumina. An increase in the time to reach equilibrium is expected as extrudates impose an additional resistance to gas diffusion independent of the binder used. The binder content affected the BET surface area to a similar degree as the water sorption capacity (Figure 5A). These changes are a consequence of the overall effect of algal biomass on the pores of alumina (Figure S14).

Similar to what we report, it is relatively common that shaping of adsorbent powders negatively affects their adsorption properties.[6] This is especially true if the binders do not provide a significant amount of macropores.[2] In the case of zeolites, substantial reductions in the adsorption capacity and diffusivity have been observed. In bentonite-

https://doi.org/10.1021/acsomega.5c00173
ACS Omega 2025, 10, 17735−17743

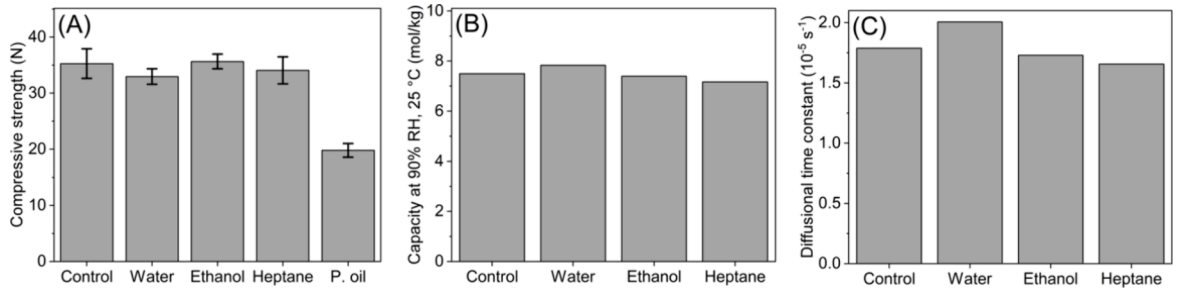

Figure 5. Comparison of Al_2O_3−Alg15 properties after a 1 week immersion in different liquids: compressive strength (A), adsorption capacity at 90% RH (B), and diffusional time constant (C).

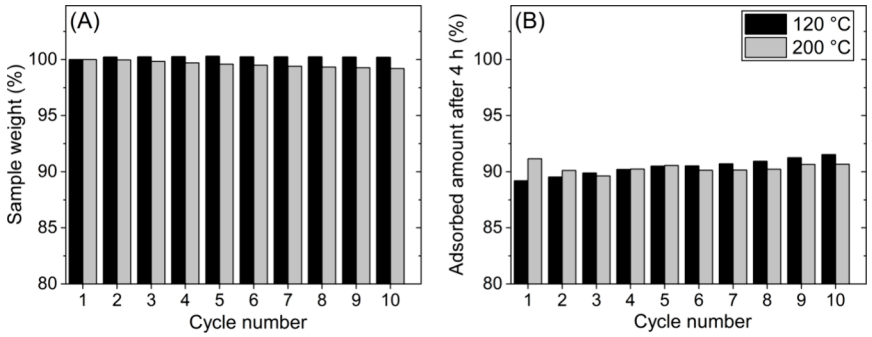

Figure 6. Comparison of Al_2O_3−Alg15 during 10 adsorption−desorption cycles at 90% RH and 25 °C with intermediate treatment at 120 and 200 °C: sample weight (A) and adsorbed amount after 4 h relative to the fresh material at equilibrium (B).

bound NaY granules, the increase in compressive strength was accompanied by a reduction in the BET surface area of 66% and in Xe diffusion of a factor of 22 compared to binderless particles.[37] In conventional and hierarchical ZSM-5, the BET surface area was found to reduce by 20−25% and the diffusivity was considerably reduced upon granulation with attapulgite or extrusion with kaolin, although this largely was due to the increase in particle size.[38] In 13X pellets, the use of several binders at 20% weight led to a 7−18% decrease in the BET surface area and up to 70% reduction in the macropore and micropore diffusion coefficients of CO_2, CH_4, and N_2.[39] The authors have not found such direct comparisons for powder vs shaped alumina adsorbents likely because it is industrially produced as powders and spheres of different particle sizes.[34]

Long-Term Stability. Samples weathered in water, ethanol, or *n*-heptane presented unaltered mechanical resistance compared to the control Al_2O_3−Alg15 material (Figure 5A). However, the sample weathered in paraffin oil still contained oil (Table S7), had diminished mechanical strength due to treatment at 200 °C in air (Figure 3), and was discarded from further study. The sample immersed in water presented a slightly higher adsorption capacity and diffusional time constant (Figure 5B,C) compared to the control sample, whereas the samples immersed in ethanol and *n*-heptane presented values very similar to those of the control. The increased capacity and diffusivity of the sample immersed in water can be related to the leaching from algal biomass. These results indicate that the formulated adsorbents are suitable for use in liquid-phase adsorption experiments.

The raw data of the gas-phase cycling experiments are presented in Figure S16. The activated sample weight and the maximum adsorbed amount reached at 4 h show the effects of cycling on the formulated adsorbents (Figure 6). When the temperature used for desorption was 200 °C, a steady decrease in adsorbent weight (0.8% after 10 cycles) was observed, which indicates degradation of the binder. Oppositely, there was a weight increase in the sample treated at 120 °C only after the first cycle, which then remained unchanged throughout the cycles. This indicates incomplete regeneration in subsequent cycles as the temperature was not high enough to completely remove adsorbed water.

After 10 cycles, one final uptake measurement was performed where equilibrium was reached. The results are summarized in Table 3. When the activation during 10 cycles was done at 120 °C, there was no significant decrease in the compressive strength. The adsorption capacity decreased by 7%, and the diffusivity was also slightly reduced. The loss in adsorption capacity matched that of the parent alumina when treated at 120 °C instead of 200 °C (SI, section 2.5), confirming that it was due to incomplete regeneration and not sample degradation. When the activation was done at 200 °C, there was a significant decline in the said properties. The decrease in compressive strength was similar to that observed when the sample was additionally treated at 200 °C in air for 8 h. This is related to degradation of the binder. At the same

Table 3. Adsorbent Properties after 11 Water Vapor Sorption Cycling Sequences with Different Activation Temperatures[a]

property	control	11th cycle, 120 °C	11th cycle, 200 °C
compressive strength (N)	35 ± 3	31.4 ± 1.5	27 ± 3
capacity at 90% RH (mol/kg)	7.49	6.95	6.77
diffusional time constant (10^{-5} s^{-1})	1.79	1.58	1.38

[a]The uptake curve of the 11th cycle was measured for 8 h, so that equilibrium was reached.

https://doi.org/10.1021/acsomega.5c00173
ACS Omega 2025, 10, 17735−17743

time, the maximum adsorption capacity decreased slightly, probably due to the decomposition products of the binder partially blocking the porosity. Regarding the time to reach equilibrium, it is difficult to estimate any changes in the diffusion path as the isotherm is very nonlinear[40,41] and the regeneration is not complete.

Perspectives of Deployment. Cell wall-deficient, genetically engineered *C. reinhardtii* spray-dried biomass is an innocuous material that can be used both as a binder and as a coplasticizer (with water) for industrial adsorbent formulations. The algal biomass needs to be crushed to a sufficiently small particle size so it can distribute evenly in the mixture with the adsorbent particles. Upon addition of water, the extrudability of the paste that is formed increases with the content of algal biomass. The threshold amount for 100% extrudability in alumina formulations is 15% algal biomass on a dry basis. This threshold may vary for different adsorbents and algal species, as the rheological properties of the pastes will vary depending on the materials' affinity toward water—ultimately affected by the presence and composition of algal cell wall polysaccharides—and their particle size.

Regarding the chosen treatment temperatures, we consider 180 °C to be optimal to stabilize the mechanical properties of the extrudates while also destroying the DNA to suitable levels to prevent the engineered transgene from escaping. Higher temperatures affect the mechanical properties of the extrudates negatively, especially in the long run, and are thus not recommended. Mild thermal treatment (110 °C, 12 h) was found to be sufficient to completely deactivate the altered genes present in the algal DNA. All of these observations converge to the conclusion that algal biomass can be a convenient binder to shape low-thermal-stability adsorbents, such as MOFs, COFs, silica, or adsorbents destined for use in liquid-phase processes or at temperatures below 120 °C.

The production method described herein aligns with the principles of sustainability and green chemistry.[42]

- High material economy, with virtually no side-products, and 100% yield achievable with the right equipment.
- The additives (algal biomass and water) are harmless and renewable resources.
- Algal biomass is an industrial waste that is used with no further processing.
- Temperatures used are relatively low.

The utilization of algal wastes in adsorbent formulations may also extend to MOFs and COFs. In this application, temperature limitations apply not only to this binder but also to the material itself, avoiding any limitations in the regeneration protocol, as in this case.

CONCLUSIONS

In this work, we demonstrate that it is possible to utilize lightly processed biological waste from *C. reinhardtii* as a binder in the production of industrially applicable alumina adsorbents. The extrudability of the adsorbent-binder-water pastes increases with the amount of binder, reaching its maximum at 15% w/w algae content, dry basis.

For this mixture, we have established a relationship between extrudability and the viscoelasticity coefficient (tan δ), in which pastes with tan $\delta > 0.4$ are completely extrudable. This relationship was determined by indirect rheological measurements. Materials containing 15% algal biomass have mechanical strengths of 30−35 N, which are comparable to those of commercial adsorbents.

This shaping procedure leads to a certain loss of water adsorption capacity. Other than the water capacity reduction by using a binder, an additional 18% of the powder adsorbent capacity is lost, possibly due to pore blockage. The shaping process makes diffusion slower, indicating that the macropore network plays a significant role in the overall diffusion path. The materials were tested for adsorption−desorption cycling, showing good regenerability if the regeneration temperature does not increase significantly above 120 °C.

The extrudates are stable upon prolonged immersion in different chemicals like water, ethanol, *n*-heptane, and paraffin oil. The mechanical properties after 1 week of immersion in those liquids did not deteriorate significantly, indicating that these materials can be used in liquid-phase applications.

ASSOCIATED CONTENT

Supporting Information

The Supporting Information is available free of charge at https://pubs.acs.org/doi/10.1021/acsomega.5c00173.

Additional information on the theoretical fundamentals, methods, and results presented in this work (PDF)

AUTHOR INFORMATION

Corresponding Author

Carlos A. Grande − *Intensification of Materials and Processes Laboratory, Physical Sciences and Engineering Division and Chemical Engineering Program, Physical Science and Engineering (PSE) Division, King Abdullah University of Science and Technology (KAUST), Thuwal 23955-6900, Saudi Arabia;* orcid.org/0000-0002-9558-5413; Email: carlos.grande@kaust.edu.sa

Authors

Eduardo Perez-Botella − *Intensification of Materials and Processes Laboratory, Physical Sciences and Engineering Division, King Abdullah University of Science and Technology (KAUST), Thuwal 23955-6900, Saudi Arabia;* orcid.org/0000-0001-5622-4693

Yesid S. Murillo-Acevedo − *Intensification of Materials and Processes Laboratory, Physical Sciences and Engineering Division, King Abdullah University of Science and Technology (KAUST), Thuwal 23955-6900, Saudi Arabia;* orcid.org/0000-0001-8911-0086

Bárbara Bastos de Freitas − *Bioengineering Program, Biological and Environmental Sciences and Engineering Division, King Abdullah University of Science and Technology (KAUST), Thuwal 23955-6900, Saudi Arabia;* orcid.org/0000-0002-5059-4383

Kyle J. Lauersen − *Bioengineering Program, Biological and Environmental Sciences and Engineering Division, King Abdullah University of Science and Technology (KAUST), Thuwal 23955-6900, Saudi Arabia;* orcid.org/0000-0002-5538-7201

Complete contact information is available at: https://pubs.acs.org/10.1021/acsomega.5c00173

Author Contributions

E.P.-B.: Conceptualization, experimental design and investigation, writing of the original draft, review and editing. Y.S.M.-A.: Conceptualization, investigation, review and editing.

https://doi.org/10.1021/acsomega.5c00173
ACS Omega 2025, 10, 17735−17743

B.B.d.F.: Investigation, review and editing. K.J.L.: Supervision, review and editing. C.A.G.: Supervision, conceptualization, review and editing. All authors have given approval to the final version of the manuscript.

Notes

The authors declare no competing financial interest.

■ ACKNOWLEDGMENTS

C. reinhardtii biomass contract cultivation was supported by the King Abdullah University of Science & Technology (KAUST) Circular Carbon Initiative grant 5213 "Scaling production of high value biochar: feedstock variability, material characterization, and field trials". K.J.L. and C.G. acknowledge KAUST Baseline Research Funding.

■ REFERENCES

(1) Yang, R. T. *Adsorbents: Fundamentals and Applications*; Yang, R. T., Ed.; Wiley-Interscience, 2003.
(2) Kraushaar-Czarnetzki, B.; Müller, S. P. Shaping of Solid Catalysts. In *Synthesis of Solid Catalysts*; De Jong, K. P., Ed.; Wiley, 2009; pp 173−199.
(3) Lawson, S.; Li, X.; Thakkar, H.; Rownaghi, A. A.; Rezaei, F. Recent Advances in 3D Printing of Structured Materials for Adsorption and Catalysis Applications. *Chem. Rev.* **2021**, *121* (10), 6246−6291.
(4) Rosseau, L. R. S.; Middelkoop, V.; Willemsen, H. A. M.; Roghair, I.; van Sint Annaland, M. Review on Additive Manufacturing of Catalysts and Sorbents and the Potential for Process Intensification. *Front. Chem. Eng.* **2022**, *4*, No. 834547.
(5) Akhtar, F.; Andersson, L.; Ogunwumi, S.; Hedin, N.; Bergström, L. Structuring Adsorbents and Catalysts by Processing of Porous Powders. *J. Eur. Ceram. Soc.* **2014**, *34* (7), 1643−1666.
(6) Wu, J.; Zhu, X.; Yang, F.; Wang, R.; Ge, T. Shaping Techniques of Adsorbents and Their Applications in Gas Separation: A Review. *J. Mater. Chem. A* **2022**, *10* (43), 22853−22895.
(7) Lakiss, L.; Gilson, J.-P.; Valtchev, V.; Mintova, S.; Vicente, A.; Vimont, A.; Bedard, R.; Abdo, S.; Bricker, J. Zeolites in a Good Shape: Catalyst Forming by Extrusion Modifies Their Performances. *Microporous Mesoporous Mater.* **2020**, *299*, No. 110114.
(8) Aranzabal, A.; Iturbe, D.; Romero-Sáez, M.; González-Marcos, M. P.; González-Velasco, J. R.; González-Marcos, J. A. Optimization of Process Parameters on the Extrusion of Honeycomb Shaped Monolith of H-ZSM-5 Zeolite. *Chem. Eng. J.* **2010**, *162* (1), 415−423.
(9) Rahul, A. V.; Sharma, A.; Santhanam, M. A Desorptivity-Based Approach for the Assessment of Phase Separation during Extrusion of Cementitious Materials. *Cem. Concr. Compos.* **2020**, *108*, No. 103546.
(10) Wang, Z.; Liu, L.; Li, Z.; Goyal, N.; Du, T.; He, J.; Li, G. K. Shaping of Metal−Organic Frameworks: A Review. *Energy Fuels* **2022**, *36* (6), 2927−2944.
(11) Liu, X.; Lim, G. J. H.; Wang, Y.; Zhang, L.; Mullangi, D.; Wu, Y.; Zhao, D.; Ding, J.; Cheetham, A. K.; Wang, J. Binder-Free 3D Printing of Covalent Organic Framework (COF) Monoliths for CO2 Adsorption. *Chem. Eng. J.* **2021**, *403*, No. 126333.
(12) Salleh, S. Z.; Awang Kechik, A.; Yusoff, A. H.; Taib, M. A. A.; Mohamad Nor, M.; Mohamad, M.; Tan, T. G.; Ali, A.; Masri, M. N.; Mohamed, J. J.; Zakaria, S. K.; Boon, J. G.; Budiman, F.; Teo, P. T. Recycling Food, Agricultural, and Industrial Wastes as Pore-Forming Agents for Sustainable Porous Ceramic Production: A Review. *J. Clean. Prod.* **2021**, *306*, No. 127264.
(13) Otero, M.; Rozada, F.; Calvo, L. F.; García, A. I.; Morán, A. Elimination of Organic Water Pollutants Using Adsorbents Obtained from Sewage Sludge. *Dyes Pigm.* **2003**, *57* (1), 55−65.
(14) Hamd, A.; Shaban, M.; AlMohamadi, H.; Dryaz, A. R.; Ahmed, S. A.; Abu Al-Ola, K. A.; Abd El-Mageed, H. R.; Soliman, N. K. Novel Wastewater Treatment by Using Newly Prepared Green Seaweed−Zeolite Nanocomposite. *ACS Omega* **2022**, *7* (13), 11044−11056.
(15) Yang, C.; Cavalcante, J.; Bastos De Freitas, B.; Lauersen, K. J.; Szekely, G. Crude Algal Biomass for the Generation of Thin-Film Composite Solvent-Resistant Nanofiltration Membranes. *Chem. Eng. J.* **2023**, *470*, No. 144153.
(16) Nakanishi, A.; Iritani, K.; Tsuruta, A.; Yamamoto, N.; Watanabe, M.; Ozawa, N.; Watanabe, M.; Zhang, K.; Tokudome, A. Fabrication of Cell Plastics Composed Only of Unicellular Green Alga Chlamydomonas reinhardtii as a Raw Material. *Appl. Microbiol. Biotechnol.* **2022**, *106* (12), 4459−4468.
(17) Wichmann, J.; Lauersen, K. J.; Kruse, O. Green Algal Hydrocarbon Metabolism Is an Exceptional Source of Sustainable Chemicals. *Curr. Opin. Biotechnol.* **2020**, *61*, 28−37.
(18) De Freitas, B. B.; Overmans, S.; Medina, J. S.; Hong, P.-Y.; Lauersen, K. J. Biomass Generation and Heterologous Isoprenoid Milking from Engineered Microalgae Grown in Anaerobic Membrane Bioreactor Effluent. *Water Res.* **2023**, *229*, No. 119486.
(19) Chen, Y. Global Potential of Algae-Based Photobiological Hydrogen Production. *Energy Environ. Sci.* **2022**, *15* (7), 2843−2857.
(20) Escapa, C.; Coimbra, R. N.; Paniagua, S.; García, A. I.; Otero, M. Nutrients and Pharmaceuticals Removal from Wastewater by Culture and Harvesting of Chlorella Sorokiniana. *Bioresour. Technol.* **2015**, *185*, 276−284.
(21) Leong, Y. K.; Chang, J.-S. Microalgae-Based Biochar Production and Applications: A Comprehensive Review. *Bioresour. Technol.* **2023**, *389*, No. 129782.
(22) Asgar Pour, Z.; Abduljawad, M. M.; Alassmy, Y. A.; Cardon, L.; Van Steenberge, P. H. M.; Sebakhy, K. O. A Comparative Review of Binder-Containing Extrusion and Alternative Shaping Techniques for Structuring of Zeolites into Different Geometrical Bodies. *Catalysts* **2023**, *13* (4), 656.
(23) Abdallah, M. N.; Wellman, G. B.; Overmans, S.; Lauersen, K. J. Combinatorial Engineering Enables Photoautotrophic Growth in High Cell Density Phosphite-Buffered Media to Support Engineered Chlamydomonas reinhardtii Bio-Production Concepts. *Front. Microbiol.* **2022**, *13*, No. 885840.
(24) Gutiérrez, S.; Wellman, G. B.; Lauersen, K. J. Teaching an Old 'Doc' New Tricks for Algal Biotechnology: Strategic Filter Use Enables Multi-Scale Fluorescent Protein Signal Detection. *Front. Bioeng. Biotechnol.* **2022**, *10*, No. 979607.
(25) DuBois, M.; Gilles, K. A.; Hamilton, J. K.; Rebers, P. A.; Smith, F. Colorimetric Method for Determination of Sugars and Related Substances. *Anal. Chem.* **1956**, *28* (3), 350−356.
(26) Marsh, J. B.; Weinstein, D. B. Simple Charring Method for Determination of Lipids. *J. Lipid Res.* **1966**, *7* (4), 574−576.
(27) Arnon, D. I. COPPER ENZYMES IN ISOLATED CHLOROPLASTS. POLYPHENOLOXIDASE IN BETA VULGARIS. *Plant Physiol.* **1949**, *24* (1), 1−15.
(28) Lichtenthaler, H. K.; Buschmann, C. Chlorophylls and Carotenoids: Measurementand Characterization by UV-VIS Spectroscopy. In *Handbook of Food Analytical Chemistry*; Wrolstad, R. E.; Acree, T. E.; Decker, E. A.; Penner, M. H.; Reid, D. S.; Schwartz, S. J.; Shoemaker, C. F.; Smith, D.; Sporns, P., Eds.; Wiley, 2005; pp 171−178.
(29) ISO 604 *Plastics - Determination of Compressive Properties*, 1993.
(30) Brunauer, S.; Emmett, P. H.; Teller, E. Adsorption of Gases in Multimolecular Layers. *J. Am. Chem. Soc.* **1938**, *60* (2), 309−319.
(31) Thommes, M.; Kaneko, K.; Neimark, A. V.; Olivier, J. P.; Rodriguez-Reinoso, F.; Rouquerol, J.; Sing, K. S. W. Physisorption of Gases, with Special Reference to the Evaluation of Surface Area and Pore Size Distribution (IUPAC Technical Report). *Pure Appl. Chem.* **2015**, *87* (9−10), 1051−1069.
(32) Barrett, E. P.; Joyner, L. G.; Halenda, P. P. The Determination of Pore Volume and Area Distributions in Porous Substances. I. Computations from Nitrogen Isotherms. *J. Am. Chem. Soc.* **1951**, *73* (1), 373−380.
(33) Saud, A. N.; Majdi, H. Sh.; Saud, S. N. Synthesis of Nano-Alumina Powder via Recrystallization of Ammonium Alum. *Cerâmica* **2019**, *65* (374), 236−239.

https://doi.org/10.1021/acsomega.5c00173
ACS Omega 2025, 10, 17735−17743

(34) Hudson, L. K.; Misra, C.; Perrotta, A. J.; Wefers, K.; Williams, F. S. Aluminum Oxide. In *Ullmann's Encyclopedia of Industrial Chemistry*; Wiley, 2000.
(35) Huang, C.-P.; Stumm, W. The Specific Surface Area of γ-Al2O3. *Surf. Sci.* **1972**, *32* (2), 287−296.
(36) Desai, R.; Hussain, M.; Ruthven, D. M. Adsorption of Water Vapour on Activated Alumina. I —- Equilibrium Behaviour. *Can. J. Chem. Eng.* **1992**, *70* (4), 699−706.
(37) Charkhi, A.; Kazemeini, M.; Ahmadi, S. J.; Ammari Allahyari, S. Effect of Bentonite Binder on Adsorption and Cation Exchange Properties of Granulated Nano NaY Zeolite. *Adv. Mater. Res.* **2011**, *335*−*336*, 423−428.
(38) Gueudré, L.; Milina, M.; Mitchell, S.; Pérez-Ramírez, J. Superior Mass Transfer Properties of Technical Zeolite Bodies with Hierarchical Porosity. *Adv. Funct. Mater.* **2014**, *24* (2), 209−219.
(39) Najafi, A. M.; Soltanali, S.; Khorashe, F.; Ghassabzadeh, H. Effect of Binder on CO2, CH4, and N2 Adsorption Behavior, Structural Properties, and Diffusion Coefficients on Extruded Zeolite 13X. *Chemosphere* **2023**, *324*, No. 138275.
(40) Cardenas, C.; Farrusseng, D.; Daniel, C.; Aubry, R. Modeling of Equilibrium Water Vapor Adsorption Isotherms on Activated Carbon, Alumina and Hopcalite. *Fluid Phase Equilib.* **2022**, *561*, No. 113520.
(41) Ribeiro, A. M.; Sauer, T. P.; Grande, C. A.; Moreira, R. F. P. M.; Loureiro, J. M.; Rodrigues, A. E. Adsorption Equilibrium and Kinetics of Water Vapor on Different Adsorbents. *Ind. Eng. Chem. Res.* **2008**, *47* (18), 7019−7026.
(42) Anastas, P. T.; Warner, J. C. *Green Chemistry: Theory and Practice*; Oxford University Press: Oxford, 2000.

https://doi.org/10.1021/acsomega.5c00173
ACS Omega 2025, 10, 17735−17743